



Detection of pancreatic ductal adenocarcinoma and liver metastases: comparison of Gd-EOB-DTPA-enhanced MR imaging vs. extracellular contrast materials

| | |
|-------|--|
| メタデータ | 言語: English 出版者: Springer Nature 公開日: 2021-04-26 キーワード: Magnetic Resonance Imaging, Pancreatic Cancer, Metastasis, Contrast Materials 作成者: Noda, Yoshifumi, Goshima, Satoshi, Takai, Yukiko, Kawai, Nobuyuki, Kawada, Hiroshi, Tanahashi, Yukichi, Matsuo, Masayuki メールアドレス: 所属: |
| URL | http://hdl.handle.net/10271/00003741 |

Detection of pancreatic ductal adenocarcinoma and liver
metastases: comparison of Gd-EOB-DTPA-enhanced MR
imaging vs. extracellular contrast materials

Original Research

Abstract

Purpose: To compare the detectability of PDAC and liver metastases between Gd-EOB-DTPA- and extracellular contrast materials (ECCMs) contrast-enhanced MR imaging contrast.

Methods: Two hundred seventy-two patients with suspected pancreatic disease underwent Gd-EOB-DTPA-enhanced MR imaging (EOB group, $n = 79$) or ECCMs-enhanced MR imaging (ECCM group, $n = 193$). The ECCM group were administered the following contrast agents: Gd-DTPA ($n = 158$), Gd-BT-DO3A ($n = 28$), Gd-DOTA ($n = 5$), and Gd-DTPA-BMA ($n = 2$). Signal intensities of pancreatic parenchyma, paraspinal muscle, PDAC (if present), and background noise were measured. The signal intensity ratio (SIR) of the pancreas and tumor-to-pancreas contrast-to-noise ratio (CNR) were also calculated. If present, the conspicuity of PDAC was evaluated with the arterial dominant phase images. Liver metastases, if present, were also evaluated for all sequences. Qualitative and quantitative imaging parameters were compared between EOB and ECCM groups.

Results: SIR of the pancreas ($P < 0.001$) and CNR ($P = 0.0037$) were significantly lower in EOB group when compared with the ECCM group. However, the sensitivity (97.1% vs. 93.5%, $P = 0.42$) and specificity (100.0% vs. 99.2%, $P = 1.00$) for detecting

PDAC were not significant between EOB and ECCM groups. The EOB group showed a significantly greater sensitivity for detecting liver metastases compared with the ECCM group (95.0% vs 84.5%, $P = 0.04$) when evaluating on a lesion-by-lesion basis.

Conclusions: Gd-EOB-DTPA-enhanced MR imaging performed similarly to ECCMs-enhanced MR imaging in detecting PDAC but had better sensitivity in detecting liver metastases.

Key Words Magnetic Resonance Imaging, Pancreatic Cancer, Metastasis, Contrast

Materials

Introduction

Pancreatic ductal adenocarcinoma (PDAC) is the fourth leading cause of cancer-related death in both males and females in the United States [1]. Despite improved diagnostic techniques and therapeutic options, PDAC has an extremely poor prognosis with a 5 year survival rate of approximately 8% for all stages [1]. Complete surgical resection is the only treatment option that benefits survival. However, less than 20% of patients have resectable tumors at the time of diagnosis [2]. The remaining patients that present with distant metastases or locally advanced tumors [3] receive chemotherapy or radiation therapy. Consequently, in order to determine the appropriate treatment option, appropriate imaging modalities are needed to accurately detect and diagnose primary tumor and distant metastases.

Gadolinium ethoxybenzyl diethylenetriamine pentaacetic acid (Gd-EOB-DTPA, Eovist[®] or Primovist[®], Bayer HealthCare, Wayne, NJ) is a liver-specific contrast material and has been reported to be useful for the detection of liver metastases in patients with PDAC [4]. As a consequence of its lower dosage, the arterial enhancement of solid organs is expected to be weaker when compared with ECCMs. A Gd-EOB-DTPA dosage of 0.025 mmol/kg body weight, approved by the Food and Drug Administration, is equivalent to a quarter of ECCMs recommended dosage. Despite the difference in dosage, we anticipate that Gd-EOB-DTPA and ECCMs will have similar

outcomes when detecting PDAC. Given this, we hypothesize that Gd-EOB-DTPA is preferred for the simultaneous evaluation of PDAC and liver metastases when compared with ECCMs. Thus, the purpose of this study was to compare the detectability of PDAC and liver metastases between Gd-EOB-DTPA- and ECCMs-enhanced magnetic resonance (MR) imaging.

Method

Patients

This retrospective study was approved by our Institutional Review Board, and written informed consent was waived. Between August 2004 and August 2018, 404 consecutive patients with known or suspected pancreatic disease based on either their clinical history or a previously performed computed tomography (CT) underwent gadolinium-enhanced MR imaging. One hundred thirty-two out of 404 patients were excluded for either the status post pancreatectomy ($n = 63$), pathologically undiagnosed ($n = 42$), severe motion artifacts ($n = 12$), absence of a complete imaging study ($n = 9$), or severe pancreatic atrophy because the radiologists could not place a region-of-interest (ROI) cursor (at least 50 mm^2) ($n = 6$). The remaining 272 patients (mean \pm SD age, 68.3 ± 10.3 years; age range, 35–84 years) were included in our study. Of these, 154

were men (mean \pm SD age, 68.5 ± 10.5 years; range, 37–84 years) and 118 were women (mean \pm SD age, 68.1 ± 10.1 years; range, 35–84 years).

PDAC was confirmed in 132 patients (73 men and 59 women) by surgery ($n = 63$) or endoscopic ultrasound-guided fine-needle aspiration ($n = 69$). None of PDAC was confirmed for the remaining 140 patients (59 men and 81 women) by CT or MR imaging performed more than 6 months after initial MR imaging. The final diagnoses in patients without PDAC were no evidence of disease ($n = 55$), branch duct-intraductal papillary mucinous neoplasm ($n = 48$), autoimmune pancreatitis ($n = 11$), chronic pancreatitis ($n = 10$), neuroendocrine tumor ($n = 2$), pancreatic metastatic tumor from renal cancer ($n = 2$), retention cyst ($n = 2$), hepatocellular carcinoma ($n = 1$), cholangiocellular carcinoma ($n = 1$), main duct-intraductal papillary mucinous neoplasm ($n = 1$), malignant lymphoma ($n = 1$), paraganglioma ($n = 1$), lymph node metastasis from gastric cancer ($n = 1$), liver metastases from ureter cancer ($n = 1$), biliary carcinoma ($n = 1$), retroperitoneal tumor ($n = 1$), and gallbladder cancer ($n = 1$).

MR Imaging Parameters

MR imaging of the pancreas was performed using a 1.5T (Intera Achieva Nova Dual; Philips Medical Systems, Best, the Netherlands) and 3T MR system (Intera Achieva Quasar Dual; Philips Medical Systems, Best, the Netherlands) using a 6-

channel torso array coil. The MR imaging protocol consisted of the following sequences: three-dimensional fat-suppressed axial T1-weighted fast field echo imaging; in-phase and opposed-phase T1-weighted axial gradient-recalled-echo imaging; respiratory-triggered two-dimensional fat-suppressed axial T2-weighted turbo spin echo imaging; and respiratory-triggered two-dimensional axial diffusion-weighted imaging with a single-shot echo-planar sequence (Table 1).

Contrast Agent Injection and Scan Protocol

Gadolinium-enhanced MR imaging was performed with one of five contrast materials, and patients were divided into two groups according to received contrast materials. For the EOB group ($n = 79$), patients received 0.025 mmol gadolinium (Gd)/kg body weight for Gd-EOB-DTPA (0.25 mmol Gd/mL; Primovist[®], Bayer HealthCare). For the ECCM group ($n = 193$), 0.1 mmol Gd/kg body weight were administered for the following contrast materials: Gd-DTPA (0.5 mmol Gd/mL; Magnevist[®], Bayer HealthCare) ($n = 158$), Gd-BT-DO3A (1.0 mmol Gd/mL; Gadovist[®], Bayer HealthCare) ($n = 28$), Gd-DOTA (0.5 mmol Gd/mL; Magnescape[®][Japan], Dotarem[®][US], Guerbet) ($n = 5$), or Gd-DTPA-BMA (0.5 mmol Gd/mL; Omniscan[®]; GE Healthcare) ($n = 2$) (Fig. 1). All contrast materials were injected at a rate of 2 mL/s followed by a 30 mL saline flush at the same rate. A multi-phase scan was initiated once

the contrast entered the abdominal aorta upon detection by a bolus-tracking technique. The arterial dominant and portal venous phases were imaged 10 and 45 s after the detection of contrast in the abdominal aorta, and late-dynamic phases were imaged 120 and 180 s after administration of contrast material. For the EOB group, hepatobiliary phase images were obtained immediately after the imaging acquisition described above (15–20 min).

Reference Standard of Liver Metastases

The study coordinator (____, with 18 years of post-training experience in interpreting abdominal images), reviewed all gadolinium-enhanced MR images, dynamic contrast-enhanced CT, and follow-up imaging studies for 132 patients with PDAC to identify liver metastases. In this review, 178 liver metastases were identified in 29 patients on the basis of pathologic results ($n = 2$); imaging findings showed hypoattenuation on post-contrast CT or MR images, hypointensity on hepatobiliary phase images, and increased size at the follow-up images ($n = 155$), or decreased size after chemotherapy at the follow-up images ($n = 21$). Among the two liver metastases which were diagnosed by pathology, one was diagnosed by preoperative liver biopsy and another one was diagnosed by intraoperative liver resection.

Quantitative Image Analysis

Two radiologists independently measured and gave consensus of the signal intensities in the arterial dominant phase images for the pancreatic parenchyma (SI_{pancreas}), paraspinal muscle, and PDAC (SI_{PDAC} , if present). For the pancreatic parenchyma, a circular or oval ROI was placed avoiding the main pancreatic ducts, focal lesions, and artifacts. For the PDAC, the signal intensity was measured within a circular or oval ROI cursor drawn on the images that encompassed most of the lesion while avoiding artifacts and large vessels. The signal intensity of the background noise (SD_{noise}) was also measured using an ROI placed outside of the body and ventral to the liver along the phase-encoding direction [5].

The signal intensity ratio (SIR) of the pancreas was calculated as a ratio of signal intensity of the pancreatic parenchyma to that of paraspinal muscle. The tumor-to-pancreas contrast-to-noise ratio (CNR) was calculated with the following equation:

$$\text{CNR} = (SI_{\text{pancreas}} - SI_{\text{PDAC}}) / SD_{\text{noise}}.$$

Image Analysis for Detecting PDAC

Image analysis was performed by two radiologists (____ and ____ with 7 and 1 years of post-training experience in abdominal image interpretation, respectively).

Radiologists were blinded to patients' clinical information or final diagnosis. They randomly and independently graded the presence or absence of PDAC using a 5-point

rating scale [4] and in consensus: 5 for definitely present, 4 for probably present, 3 for equivocal, 2 for probably absent, and 1 for definitely absent (Fig. 2). A confidence rating of 3–5 indicated PDAC. If PDAC was considered to be present, radiologists recorded the location of each lesion.

Image Analysis for Detecting Liver Metastases

For the patients with PDAC, radiologists independently graded the diagnostic confidence of liver metastases using a 5-point rating scale for each liver lesion and in consensus: 5 for definitely present, 4 for probably present, 3 for equivocal, 2 for probably absent, and 1 for definitely absent (Fig. 3). A confidence rating of 3–5 indicated the presence of liver metastases. If liver metastases were considered to be present, the maximal diameter for each lesion was recorded.

Statistical Analysis

Statistical analyses were performed using MedCalc Software for Windows (version 19.0.5, Mariakerke, Belgium). The Mann–Whitney U and Fisher’s exact test were completed to evaluate statistical differences in patient age, sex, maximal diameter of PDAC, location of PDAC, TNM stages, stage classification, maximal diameter of liver metastases, SIR of the pancreas, and CNR between the EOB and ECCM groups. The sensitivity, specificity, positive predictive value (PPV), and negative predictive

value (NPV) for detecting PDAC and liver metastasis were compared between EOB and ECCM groups using the Fisher's exact tests. For each group, receiver-operating-characteristic (ROC) curves were fitted to confidence ratings for detecting PDAC. A patient was selected as positive when at least one liver metastasis was radiologically identified. Lesion-by-lesion analyses were also conducted for all lesions and less than 10 mm in maximal diameter, respectively. A P value of < 0.05 was considered statistically significant. To assess interobserver variability in the confidence ratings for detecting PDAC and liver metastases, and quantitative measurements, κ statistics and intraclass correlation coefficient (ICC) were used to measure the degree of interobserver agreement. A κ value and an ICC of up to 0.20 were interpreted as slight agreement, 0.21–0.40 as fair agreement, 0.41–0.60 as moderate agreement, 0.61–0.80 as substantial agreement, and ≥ 0.81 as almost in complete agreement.

Results

Patient demographics and tumor characteristics

Patient demographics and tumor characteristics for both groups are summarized in Table 2. No significant differences were observed in patient age ($P = 0.19$), sex ($P = 0.50$), maximal diameter of PDAC ($P = 0.70$), location of PDAC ($P =$

0.58), T stage ($P = 0.56$), N stage ($P = 0.31$), M stage ($P = 0.12$), stage classification ($P = 0.23$), and maximal diameter of liver metastasis ($P = 0.064$) between EOB and ECCM groups.

Quantitative Image Analysis

The mean (\pm SD) SIR of the pancreas was significantly lower in the EOB group (2.67 ± 0.75 ; range, 0.39–4.98) than in ECCM group (3.33 ± 1.08 ; range, 0.47–6.70) ($P < 0.001$). The mean CNR (\pm SD) was significantly lower in EOB group (63.3 ± 51.6 ; range, 12.8–253.5) than in ECCM group (98.1 ± 77.0 ; range, 12.4–299.8) ($P = 0.0037$) (Fig. 4). The SIR of the pancreas (ICC, 0.69) and CNR (ICC, 0.71) interobserver variability was in substantial agreement.

Image Analysis for Detecting PDAC

No significant differences were observed in the sensitivities ($P = 0.42$), specificities ($P = 1.00$), PPVs ($P = 0.46$), and NPVs ($P = 0.07$) between the EOB and ECCM groups. The area under the ROC curves was similar between the EOB (0.998; 95% confidence interval [CI], 0.952–1.000) and the ECCM (0.994; 95% CI, 0.971–1.00) groups (Table 3, Fig. 5).

PDACs less than 10 mm in maximal diameter were not radiologically observed in either group. One false-positive case in the ECCM group was eventually diagnosed

as autoimmune pancreatitis.

The κ value in the confidence ratings for detecting PDAC was 0.711 (95% CI, 0.662–0.760). This κ value indicates substantial agreement between the two radiologists.

Image Analysis for Detecting Liver Metastases

A patient-by-patient analysis showed no significant differences in the sensitivities ($P = 0.22$), specificities ($P = 1.00$), PPVs ($P = 1.00$), and NPVs ($P = 0.57$) between the EOB and the ECCM groups. A lesion-by-lesion analysis demonstrated that the sensitivity for detecting liver metastases was significantly greater in the EOB group than in the ECCM group (95.0% for EOB group vs. 84.5% for ECCM group, $P = 0.04$). There was no significant difference in PPV between groups ($P = 0.09$). For lesions less than 10 mm in maximal diameter, a lesion-by-lesion analysis demonstrated that the sensitivity (93.8% for EOB group vs. 77.8% for ECCM group, $P = 0.02$) and PPV (100.0% for EOB group vs. 91.3% for ECCM group, $P = 0.04$) were significantly greater in EOB group than in ECCM group (Table 4, Fig. 6).

All false-negative lesions ($n = 6$) in the EOB group were less than 10 mm in maximal diameter. Similarly, in ECCM group, almost all false-negative lesions ($n = 6$) were less than 10 mm in maximal diameter. Two out of three of the remaining lesions

were 10.5 mm and 11.6 mm in and close to the maximal diameter threshold. The remaining lesion was misdiagnosed as an arterio-portal shunt. All false-positive lesions ($n = 2$) were also less than 10 mm in maximal diameter and were misdiagnosed as tiny hemangiomas. The κ value in the confidence ratings for detecting liver metastases was 0.737 (95% CI, 0.604–0.871). This κ value indicates substantial agreement between the two radiologists.

Discussion

In the present study, although the mean SIR of the pancreas and CNR were significantly lower in EOB group than in ECCM group, the diagnostic performance for detecting PDAC and liver metastases on a patient-by-patient basis were similar between groups. However, a lesion-by-lesion analysis, especially lesions less than 10 mm in maximal diameter, demonstrated that the sensitivity and PPV of detecting liver metastases were significantly greater in EOB group than in ECCM group. We sometimes experience both ECCM and Gd-EOB-DTPA are used for the evaluation of PDAC and liver metastases in same patient. Gd-EOB-DTPA-enhanced MR imaging is cost-effective for evaluating hepatocellular carcinoma or liver metastasis from colorectal cancer compared with ECCMs-enhanced MR imaging and contrast-enhanced CT [6-8]. Our study is the first attempt to evaluate the diagnostic performance in

detecting both PDAC and liver metastases in Gd-EOB-DTPA- and ECCMs-enhanced MR imaging. We believe that Gd-EOB-DTPA-enhanced MR imaging is the preferred imaging modality in patients with PDAC.

Gd-EOB-DTPA-enhanced MR imaging has shown excellent diagnostic performance of detecting liver metastases when compared with dynamic contrast-enhanced CT in patients with PDAC [4, 9]. We believed that ECCMs-enhanced MR imaging has similar diagnostic performance for detecting liver metastases as dynamic contrast-enhanced CT because iodine contrast material and ECCMs are extracellular contrast materials. This means that there is no question of the utility of Ga-EOB-DTPA-enhanced MR imaging for detecting liver metastases. The incidence of liver metastasis in patients with resectable PDAC was 10%–12% [10, 11]. Patients could avoid unnecessary surgery if small liver metastases could be preoperatively diagnosed with Ga-EOB-DTPA-enhanced MR imaging.

The ECCMs, including Gd-DTPA, Gd-BT-DO3A, Gd-DOTA, and Gd-DTPA-BMA, are established and have been used for more than two decades. Ga-EOB-DTPA have become available for the detection and characterization of focal liver lesions and have shown good diagnostic performance in hepatocellular carcinoma and liver metastases from colorectal cancer or PDAC [4, 9, 12-14]. Previous studies reported that

contrast enhancement of abdominal solid organs and major vessels is weaker in Ga-EOB-DTPA when compared with other ECCMs [15, 16]. When compared with other ECCMs (4.2–5.3), Ga-EOB-DTPA has high T1 relaxivity (7.3) in 37°C human blood at 1.5T [17]. However, because of only one-quarter of the dosage compared with ECCMs, Previous studies have shown that the enhancement effect of Ga-EOB-DTPA is weaker and is likely due to a low administered dose when compared with ECCMs. However, normal pancreatic parenchyma appears to be relatively hyperintense on fat-suppressed T1-weighted images. This is due to the presence of abundant glycoproteins and endoplasmic reticulum in the pancreatic tissue. These features are likely due to T1-shortening [18]. Consequently, fat-suppressed T1-weighted images may not require a significant enhancement in contrast to detect PDAC [4]. Actually, the diagnostic performance for detecting PDAC was comparable between the EOB and the ECCM groups despite the fact that the mean SIR of the pancreas was significantly lower in EOB group when compared with ECCM group in this study.

The present study has some limitations. First, this study was a retrospective design using a relatively small sample especially patients who don't have PDAC in EOB group. The NPV for the diagnosis of PDAC in EOB group was low (9/11, 81.8%), compared with those in ECCM group (130/134, 97.0%), however, the parameter was

absolutely small. We believe that this NPV is not true value of EOB group. Second, the pathological proof of liver metastases was not obtained for most of the lesions. Third, we did not compare the diagnostic performance in detecting liver metastases between Gd-EOB-DTPA-enhanced MR imaging and diffusion weighted imaging (DWI). However, a previous study concluded that addition of DWI to Gd-EOB-DTPA-enhanced MR imaging don't significantly increase diagnostic accuracy as compared to Gd-EOB-DTPA-enhanced MR imaging alone for the diagnosis of liver metastases [19]. Finally, we could not directly evaluate the diagnostic performance of detecting PDAC and liver metastases since we did not recruit the patients who completed Gd-EOB-DTPA- and ECCMs-enhanced MR imaging. Therefore, further clinical studies are prospectively required to validate our results.

In conclusion, Gd-EOB-DTPA-enhanced MR imaging was comparable with ECCMs-enhanced MR imaging in detecting PDAC and demonstrated better sensitivity in detecting liver metastases, especially for lesions less than 10 mm in maximal diameter.

Conflict of Interest

Author disclosure of potential conflict of interest. No relevant conflicts of interest to disclose.

References

1. Siegel RL, Miller KD, Jemal A. Cancer statistics, 2018. *CA Cancer J Clin* 2018; 68:7-30
2. Willett CG, Czito BG, Bendell JC, Ryan DP. Locally advanced pancreatic cancer. *J Clin Oncol* 2005; 23:4538-4544
3. Pollom EL, Koong AC, Ko AH. Treatment Approaches to Locally Advanced Pancreatic Adenocarcinoma. *Hematol Oncol Clin North Am* 2015; 29:741-759
4. Motosugi U, Ichikawa T, Morisaka H, et al. Detection of pancreatic carcinoma and liver metastases with gadoxetic acid-enhanced MR imaging: comparison with contrast-enhanced multi-detector row CT. *Radiology* 2011; 260:446-453
5. van Kessel CS, Veldhuis WB, van den Bosch MA, van Leeuwen MS. MR liver imaging with Gd-EOB-DTPA: a delay time of 10 minutes is sufficient for lesion characterisation. *Eur Radiol* 2012; 22:2153-2160
6. Suh CH, Kim KW, Park SH, et al. Performing Gadoxetic Acid-Enhanced MRI After CT for Guiding Curative Treatment of Early-Stage Hepatocellular Carcinoma: A Cost-Effectiveness Analysis. *AJR Am J Roentgenol* 2018; 210:W63-W69
7. Nishie A, Goshima S, Haradome H, et al. Cost-effectiveness of EOB-MRI for

Hepatocellular Carcinoma in Japan. *Clin Ther* 2017; 39:738-750 e734

8. Zech CJ, Justo N, Lang A, et al. Cost evaluation of gadoxetic acid-enhanced magnetic resonance imaging in the diagnosis of colorectal-cancer metastasis in the liver: Results from the VALUE Trial. *Eur Radiol* 2016; 26:4121-4130
9. Ito T, Sugiura T, Okamura Y, et al. The diagnostic advantage of EOB-MR imaging over CT in the detection of liver metastasis in patients with potentially resectable pancreatic cancer. *Pancreatology* 2017; 17:451-456
10. Contreras CM, Stanelle EJ, Mansour J, et al. Staging laparoscopy enhances the detection of occult metastases in patients with pancreatic adenocarcinoma. *J Surg Oncol* 2009; 100:663-669
11. Maithel SK, Maloney S, Winston C, et al. Preoperative CA 19-9 and the yield of staging laparoscopy in patients with radiographically resectable pancreatic adenocarcinoma. *Ann Surg Oncol* 2008; 15:3512-3520
12. Hammerstingl R, Huppertz A, Breuer J, et al. Diagnostic efficacy of gadoxetic acid (Primovist)-enhanced MRI and spiral CT for a therapeutic strategy: comparison with intraoperative and histopathologic findings in focal liver lesions. *Eur Radiol* 2008; 18:457-467
13. Ooka Y, Kanai F, Okabe S, et al. Gadoxetic acid-enhanced MRI compared with

- CT during angiography in the diagnosis of hepatocellular carcinoma. *Magn Reson Imaging* 2013; 31:748-754
14. Lowenthal D, Zeile M, Lim WY, et al. Detection and characterisation of focal liver lesions in colorectal carcinoma patients: comparison of diffusion-weighted and Gd-EOB-DTPA enhanced MR imaging. *Eur Radiol* 2011; 21:832-840
 15. Ringe KI, Boll DT, Husarik DB, Bashir MR, Gupta RT, Merkle EM. Lesion detection and assessment of extrahepatic findings in abdominal MRI using hepatocyte specific contrast agents--comparison of Gd-EOB-DTPA and Gd-BOPTA. *BMC Med Imaging* 2013; 13:10
 16. Tamada T, Ito K, Sone T, et al. Dynamic contrast-enhanced magnetic resonance imaging of abdominal solid organ and major vessel: comparison of enhancement effect between Gd-EOB-DTPA and Gd-DTPA. *J Magn Reson Imaging* 2009; 29:636-640
 17. Rohrer M, Bauer H, Mintorovitch J, Requardt M, Weinmann HJ. Comparison of magnetic properties of MRI contrast media solutions at different magnetic field strengths. *Invest Radiol* 2005; 40:715-724
 18. Winston CB, Mitchell DG, Outwater EK, Ehrlich SM. Pancreatic signal intensity on T1-weighted fat saturation MR images: clinical correlation. *J Magn Reson*

Imaging 1995; 5:267-271

19. Donati OF, Fischer MA, Chuck N, Hunziker R, Weishaupt D, Reiner CS.
Accuracy and confidence of Gd-EOB-DTPA enhanced MRI and diffusion-weighted imaging alone and in combination for the diagnosis of liver metastases.

Eur J Radiol 2013; 82:822-828

Figure Captions

Fig. 1. Flow chart of the included and excluded patients.

Fig. 2. Confidence ratings for detecting pancreatic ductal adenocarcinoma (PDAC) (arrows). **(a)** 1, definitely absent; **(b)** 2, probably absent (branch duct-intraductal papillary mucinous neoplasm); **(c)** 3, equivocal (PDAC); **(d)** 4, probably present (PDAC); and **(e)** 5, definitely present (PDAC).

Fig. 3. Confidence ratings for detecting liver metastasis (arrows). **(a)** 1, definitely absent; **(b)** 2, probably absent (hemangioma); **(c)** 3, equivocal (liver metastasis); **(d)** 4, probably present (liver metastasis); and **(e)** 5, definitely present (liver metastases).

Fig. 4. Box plot showing **(a)** the signal intensity ratio (SIR) of the pancreas and **(b)** tumor-to-pancreas contrast-to-noise ratio (CNR) in the EOB and the ECCM groups. The SIR of the pancreas ($P < 0.001$) and CNR ($P = 0.0037$) were significantly lower in EOB group than in ECCM group.

Fig. 5. (a) A 74-year-old man with pancreatic ductal adenocarcinoma of the head (arrow) acquired with Gd-DTPA and **(b)** a 63-year-old man with pancreatic ductal adenocarcinoma of the head (arrow) acquired with Gd-EOB-DTPA. Representative images of the pancreatic head ductal adenocarcinoma are shown for both the cases.

Fig. 6. Liver metastases less than 10 mm in maximal diameter may be accurately detected with Gd-EOB-DTPA.

Eligible patients

404 patients with suspected of having pancreatic disease underwent contrast-enhanced MR imaging with Gd-EOB-DTPA or ECCMs.

Excluded patients ($n = 132$)

s/p pancreatectomy ($n = 63$)

Pathologically undiagnosed cases ($n = 42$)

Severe artifact ($n = 12$)

Lack of adequate images ($n = 9$)

Severe pancreatic atrophy ($n = 6$)

Remaining **272** patients (154 men and 118 women; age range, 35–84 years; mean, 68.3 ± 10.3 years) were included in our study

EOB group
($n = 79$)

ECCM group
($n = 193$)

Gd-DTPA ($n = 158$)

Gd-BT-DO3A ($n = 28$)

Gd-DOTA ($n = 5$)

Gd-DTPA-BMA ($n = 2$)

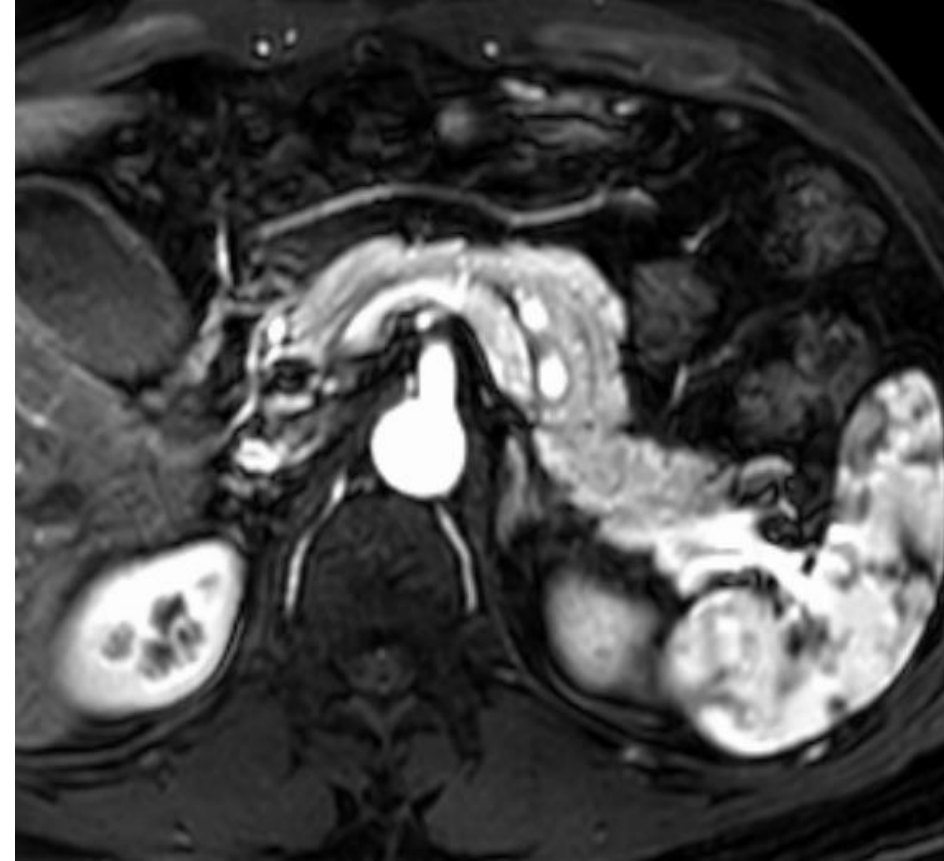


Figure 2a

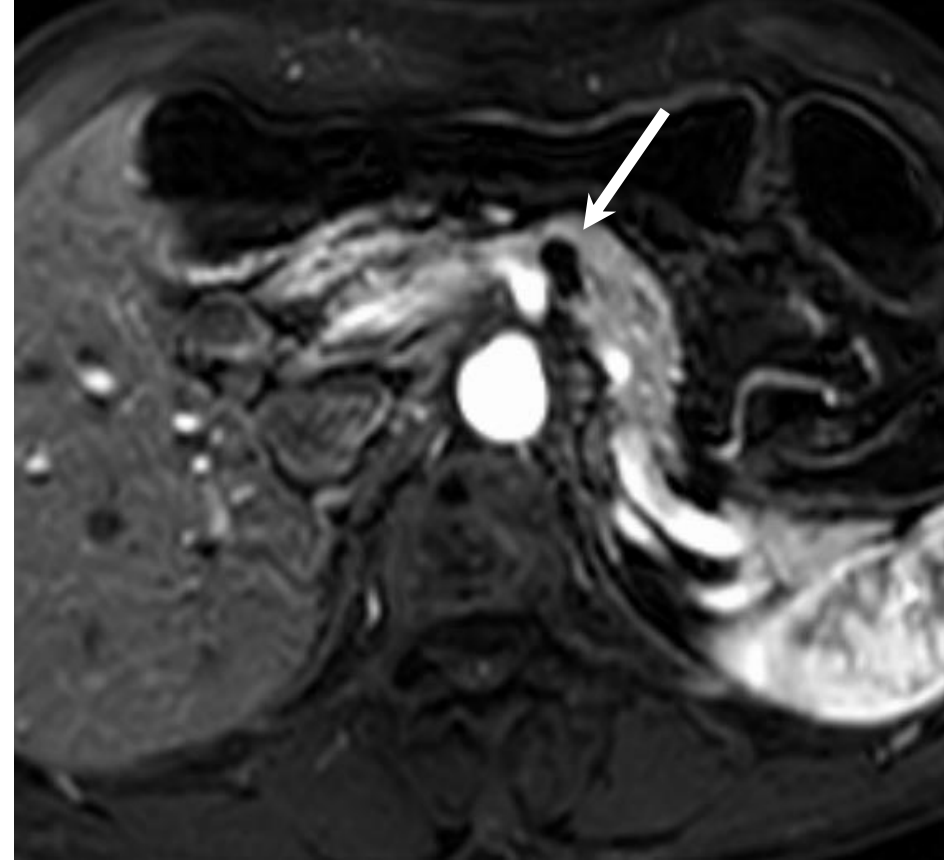


Figure 2b

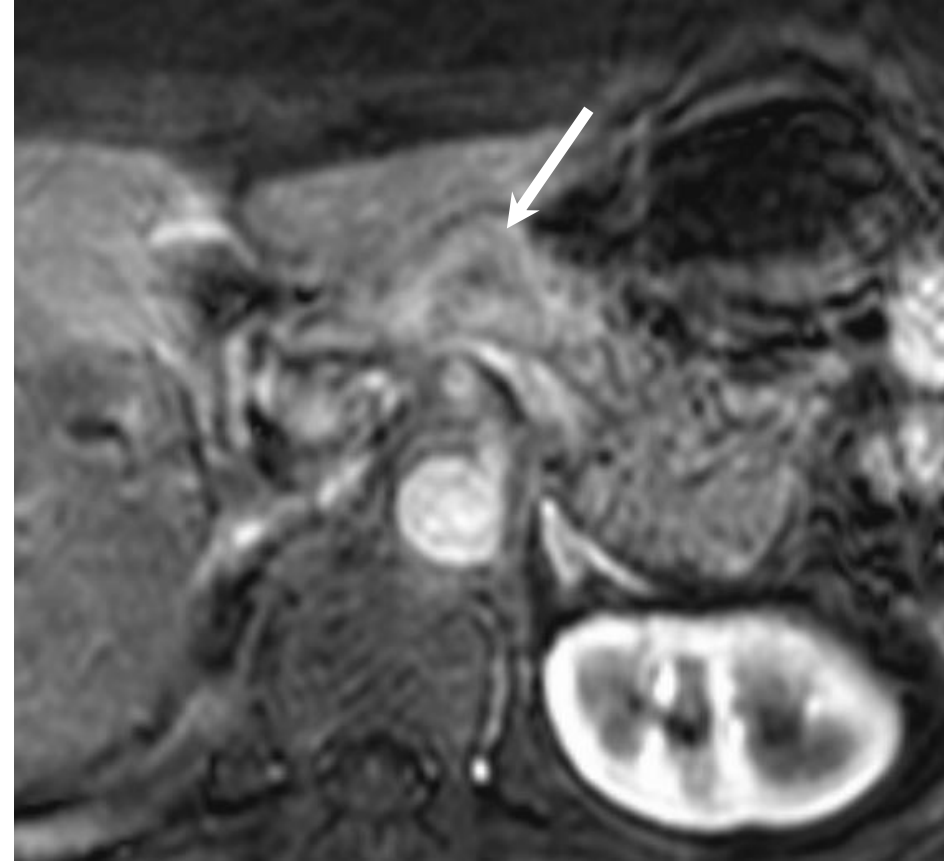


Figure 2c

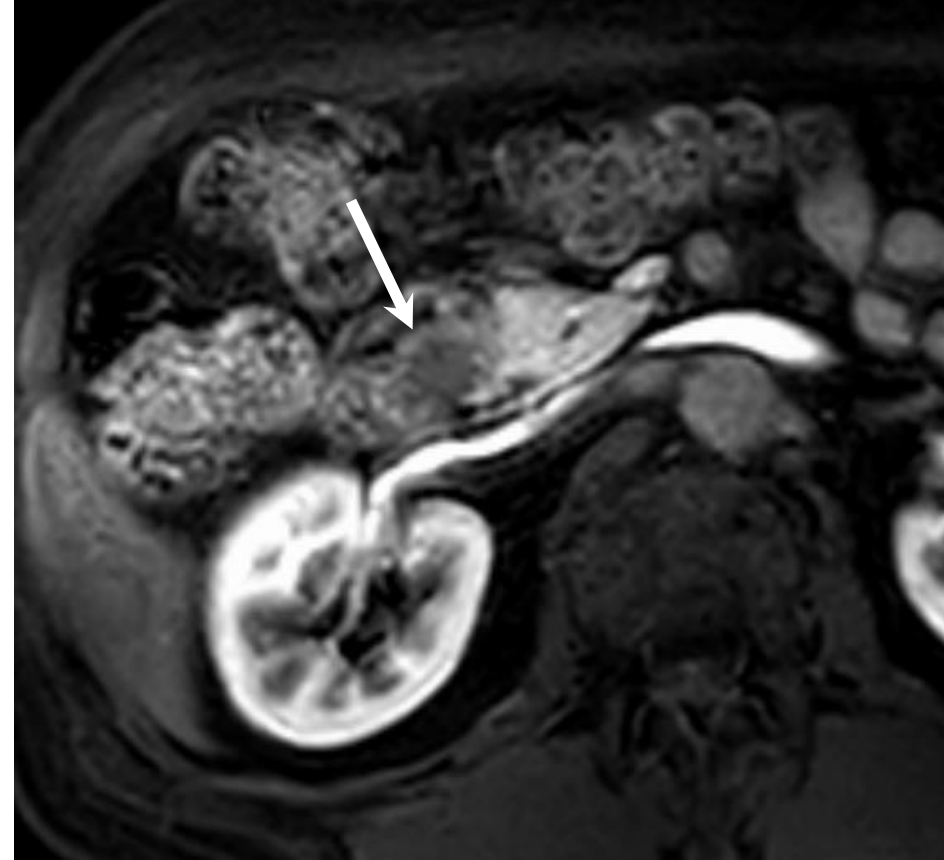


Figure 2d



Figure 2e

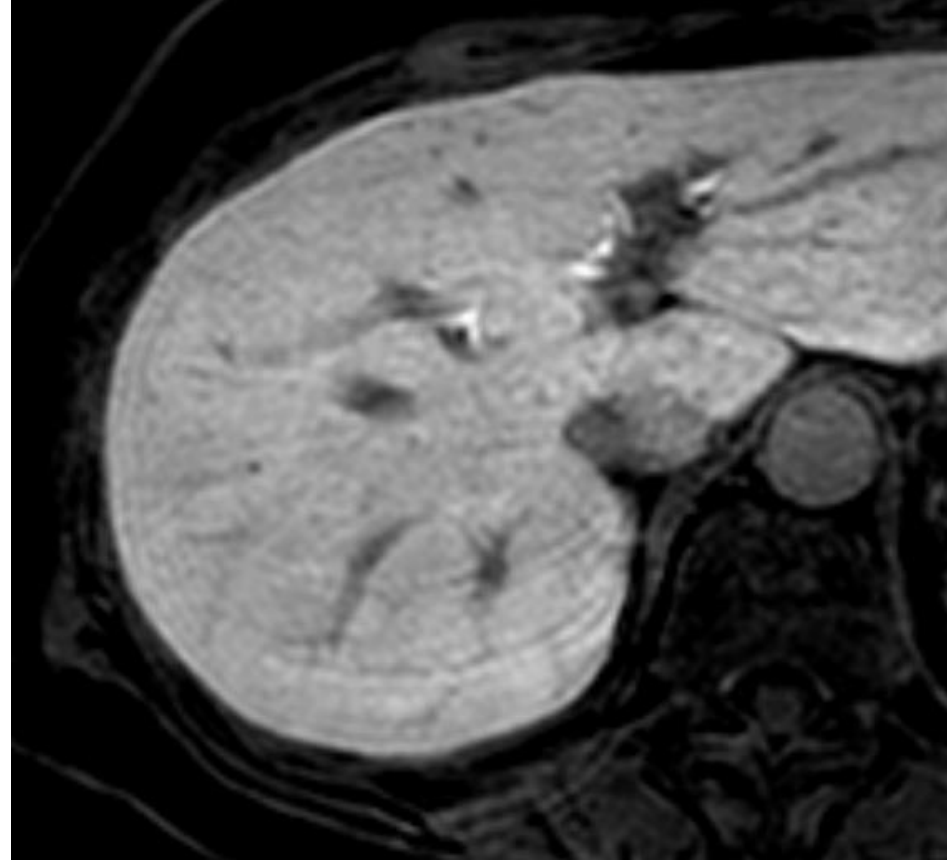


Figure 3a



Figure 3b

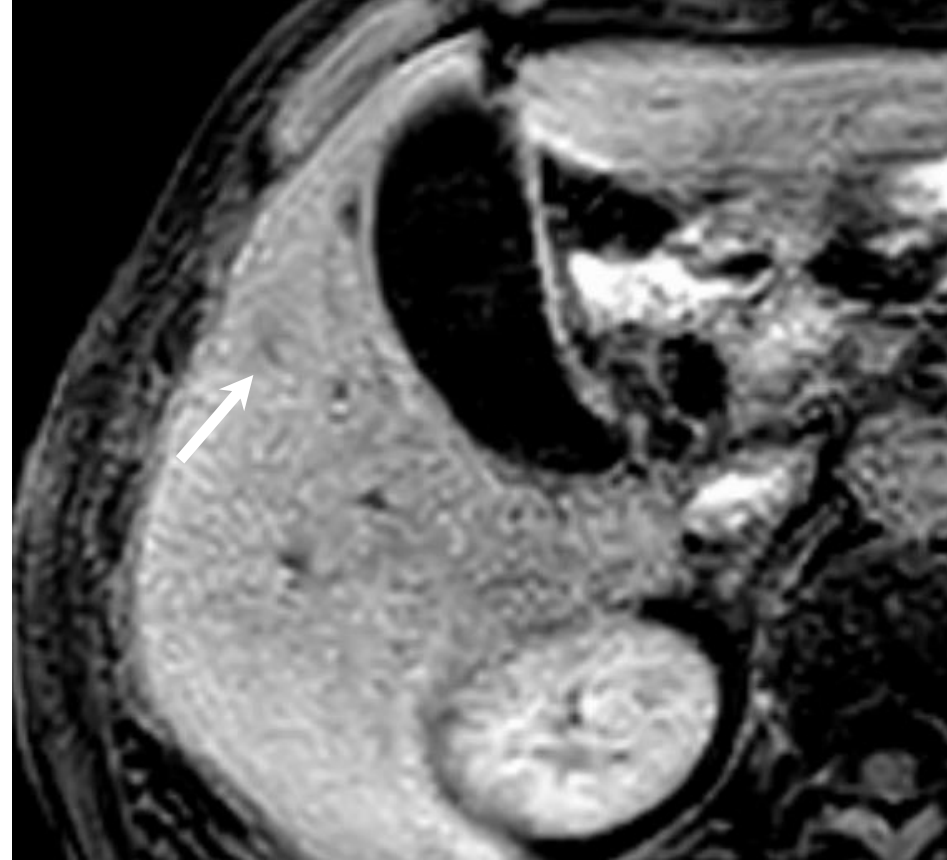


Figure 3c

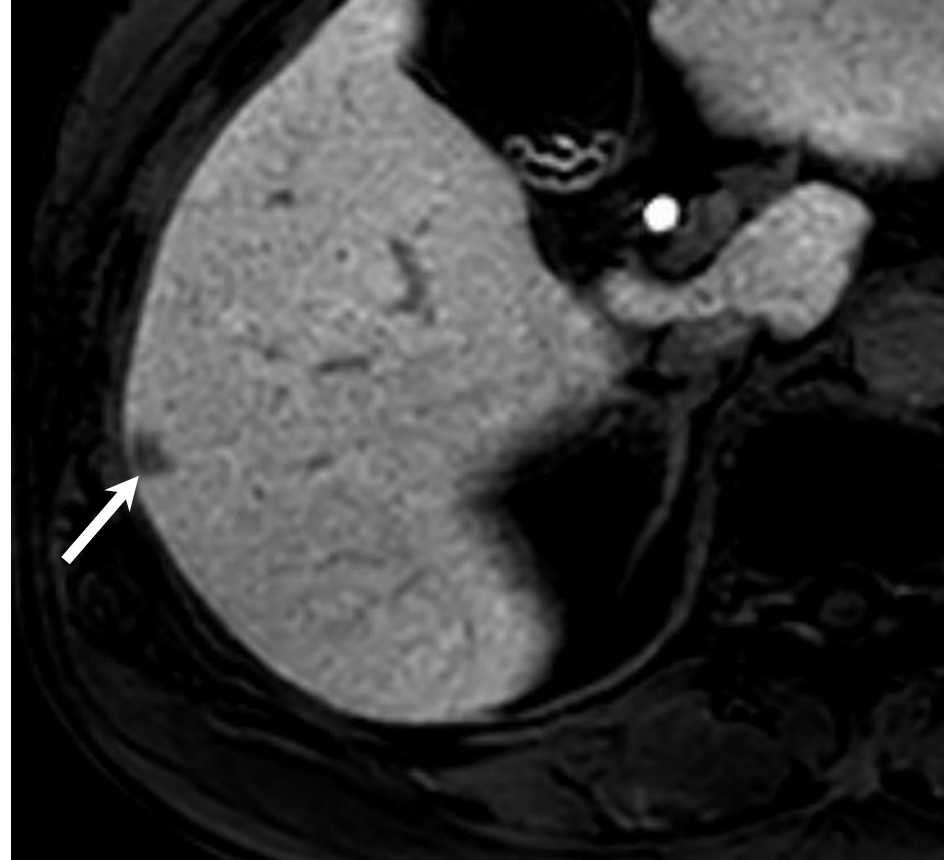


Figure 3d

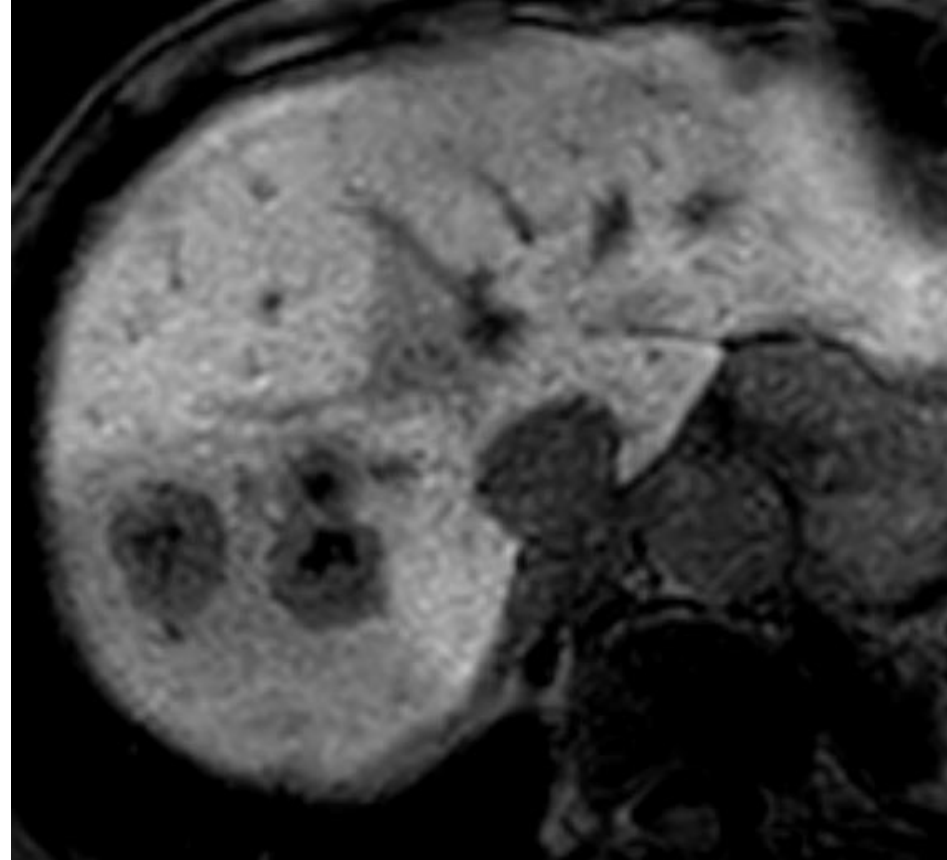


Figure 3e

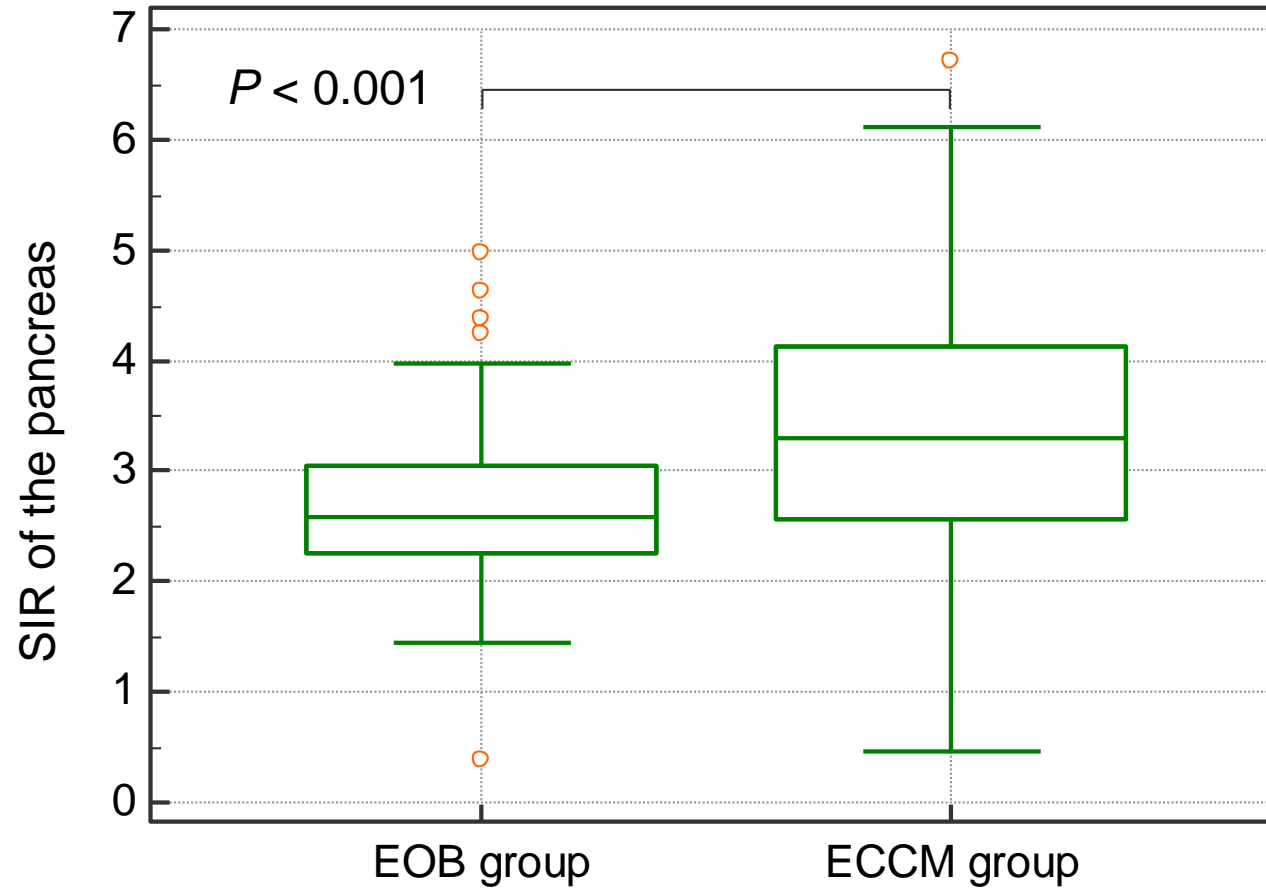


Figure 4a

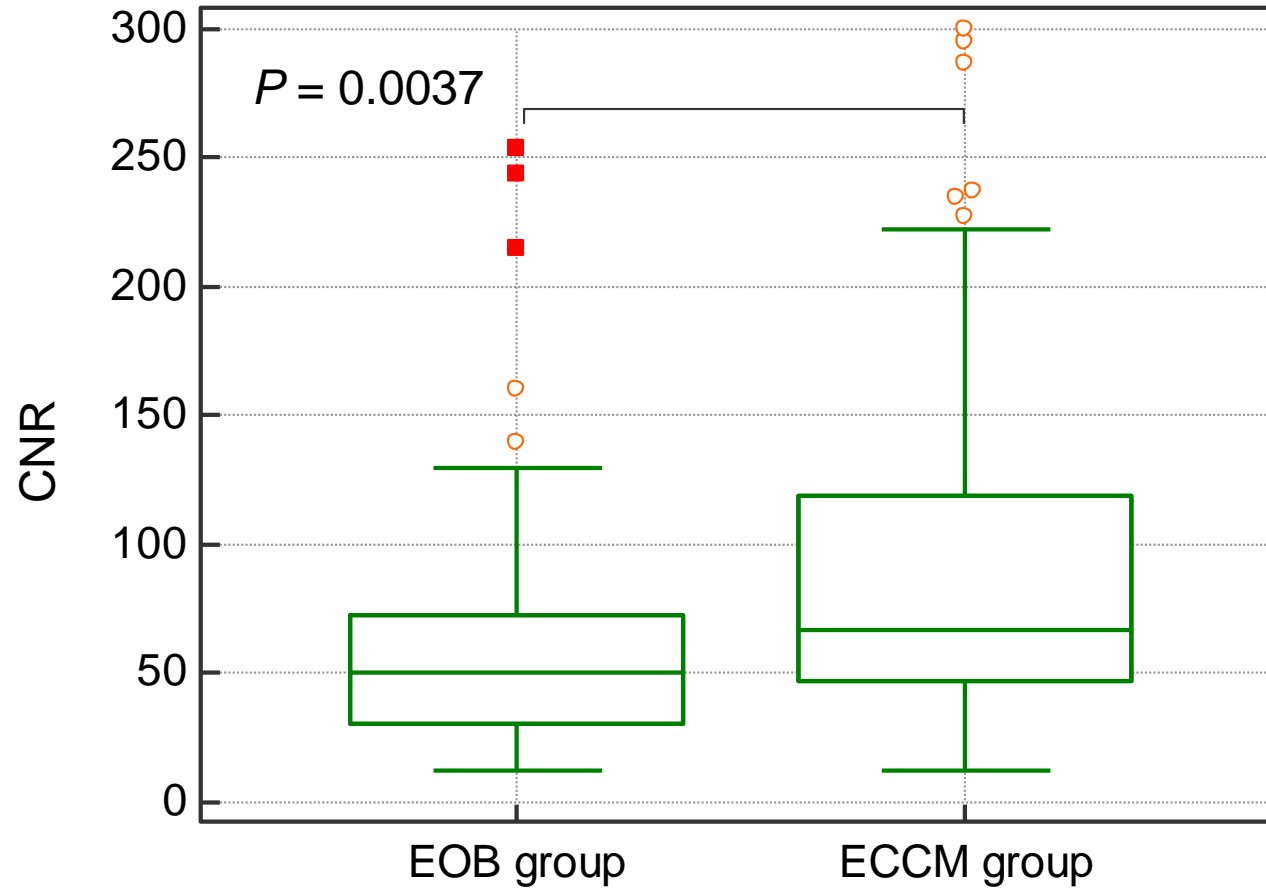


Figure 4b

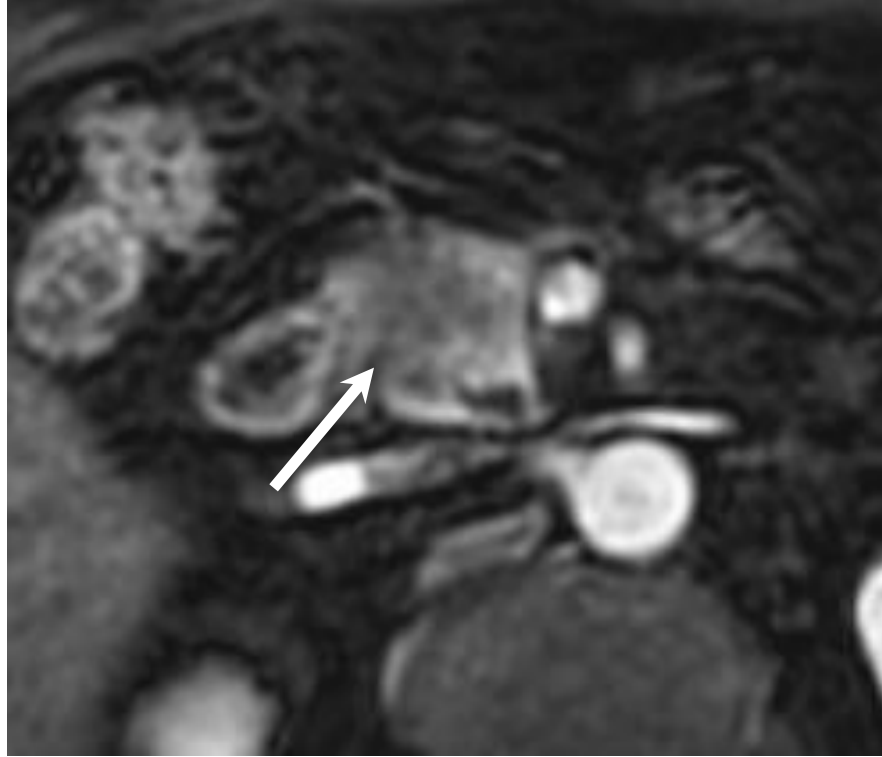


Figure 5a



Figure 5b



Figure 6a

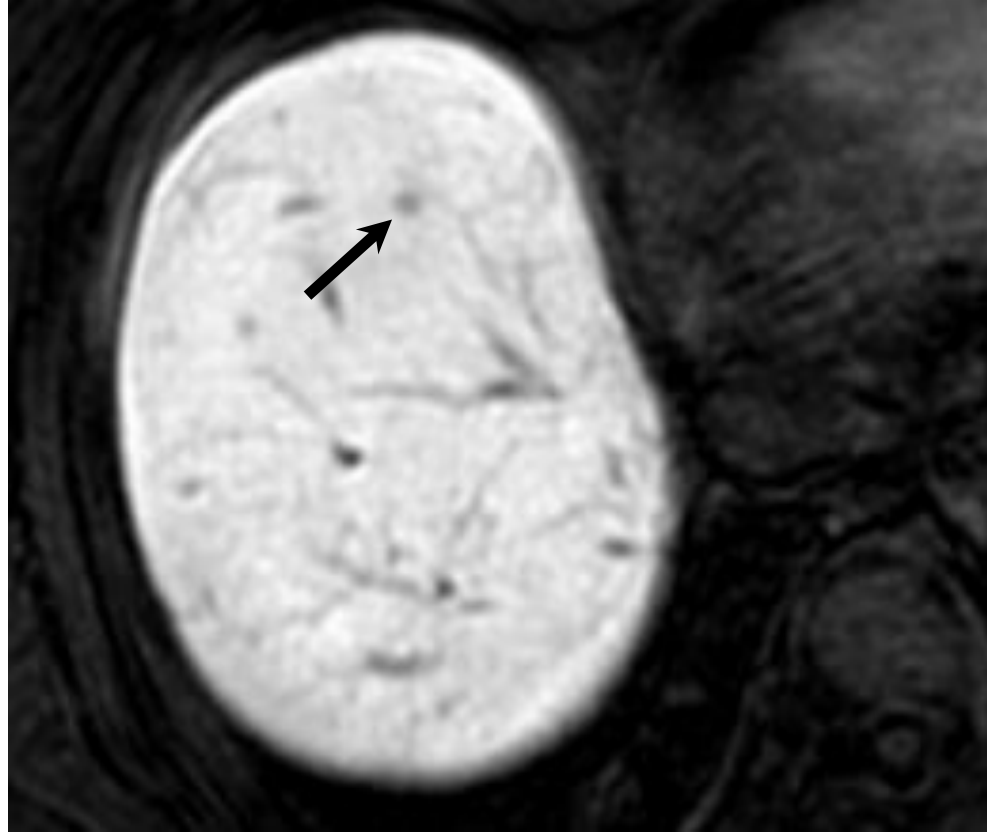


Figure 6b